2014 IEEE International Conference on Robotics & Automation (ICRA)
Hong Kong Convention and Exhibition Center
May 31 - June 7, 2014. Hong Kong, China

Development of a Symmetrical Spiral Wireless Microrobot in Pipe for Biomedical Applications

Shuxiang Guo, Xiang Wei, Jian Guo, Wei Wei, Yuehui Ji and Yunliang Wang

***Abstract*—Colonoscopy is an important procedure for the diagnosis of various pathologies, in particular cancer of the colon and of the rectum. However, colonoscopy is a procedure often painful for the patient and complex for the doctor. So in the biomedical field, a wireless microrobot in pipe that can move smoothly in water or aqueous medium has urgently been demanded. In this paper, we developed a new kind of wireless microrobot with symmetrical spiral structure, which also had symmetrical kinematic characteristics. According to the hydromechanical lubrication theory and Newton viscous law, we build the motion model of the microrobot, which will provide a theoretical basis on designing the optimal structure parameters of the microrobot. Through analysis, simulations and experiments, this paper had evaluated the effect of spiral angle, which could realize forward-backward, upward-downward motion and stopping at any position we need in the pipe. In addition, we obtained the moving speeds of forward-backward and upward-downward motion in the pipe. The experimental results indicated that the maximum moving speed is 36.5 mm/s at 14 Hz in the horizontal direction and 4.6 mm/s at 16Hz in the vertical direction with input currents of 0.7A. Finally, we designed a control panel for this system, which can control the microrobot current motion states intuitively and easily, and make our system more portable and compact. The developed wireless microrobot can move smoothly in water and other liquid medium and is very useful in the industrial application and microsurgery application.**

I. Introduction

Endovascular intervention has become more and more popular in recently. It is widely used in biomedical practice, diagnosis and surgery. Pipeline micro-robot is an important research branch of MEMS (Micro-Electro-Mechanical System). It consists of two aspects. One is to walk in the hard pipe, which is widely used in many fields of the chemical engineering, nuclear power plant and refrigeration. The other one is to walk in the flexible pipe, such as the human gastrointestinal (GI) tract, the blood vessel, for biomedical treatment. With the development of MEMS technology, make the micro-robot which is as a tool in very small spaces, and in biomedical practice, possible to enter the body and execute non-invasive or minimally invasive biomedical operations. In biomedical and industrial applications, a new type of microrobot in a pipe has urgently been needed [1]-[2]. They can move smoothly in water or other liquid medium, making it suitable for pipe inspection and microsurgery of blood vessels. To minimize the suffering of a patient, a capsule endoscope has been developed [3]. However, the capsule cannot control its moving direction and moving speed itself, due to the waste of large quantities of data. So the capsule endoscope needs an autonomous moving function.

In our previous study, as wireless microrobots controlled by a external magnetic field are both safe and reliable, and can be carried deep within the tissues of living organisms in the body fluids, it is need to propose a new kind of magnetic field model to drive the microrobot easily [4]-[6].

Recently, several types of microrobots utilizing the magnetic actuators have been developed. Honda developed a new kind of wireless swimming robot with a tail fin which can swim in one direction [7]. Thereafter Mei Tao developed another kind of wireless microrobot with desirable experiment results by using a new kind of intelligent magnetic material FMP [8]. Nokata developed new magnetic rotational drive by use of magnetic particles with specific gravity smaller than a liquid [9]. And especially Professor Guo et al developed a novel type of wireless swimming robot with a fin-driven that can move in horizontal direction and vertical direction [10]-[11]. Then they proposed more kinds of microrobots with hybrid motions, such as padding motion, propeller-driven, spiral motion [12]-[17]. In our study, previous researchers have developed several kinds of wireless microrobots as shown in Fig. 1.

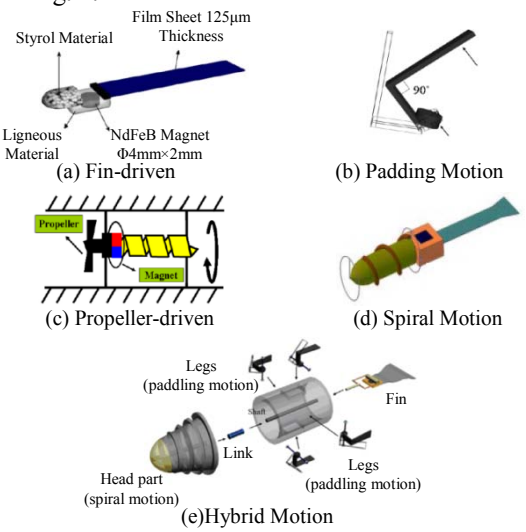

Figure 1. Several kinds of wireless microrobots

Shuxiang Guo is with the Intelligent Mechanical Systems Engineering Department, Kagawa University, Takamatsu, Kagawa, Japan. He is also with Tianjin Key Laboratory for Control Theory & Application in Complicated Systems and Biomedical Robot Laboratory, the School of Electrical Engineering, TianJin University of Technology, TianJin, China (e-mail: guo@eng.kagawa-u.ac.jp).

Xiang Wei, Jian Guo, Wei Wei, Yuehui Ji and Yunliang Wang is with Tianjin Key Laboratory for Control Theory & Application in Complicated Systems and Biomedical Robot Laboratory, the School of Electrical Engineering, TianJin University of Technology, TianJin, China (e-mail: gj15102231710@163.com; weixiang_tjut@163.com).

In the hybrid motions, the kind of spiral motion can not only obtain the maximum driving force, but also is the highest efficiency in a very small space. So we need develop a kind of microrobots with a symmetrical spiral structure immediately.

II. Modeling and Analysis of the Microrobot

A. The modeling of the microrobot

According to the right-hand rule, we established the coordinate system for the microrobot movement as shown in Fig. 2. In the right-hand coordinate system, V is the axial velocity, U is the circumferential velocity. For the sake of analysis the force effect of the microrobot, we assumed the direction of the screw thread is x-axis, the thickness direction of the screw thread is y-axis, the direction which is vertical to the microrobot body is z-axis, and θ is the spiral angle. U and V can be composed of u_x (x-component) and w_z (z-component).

$$u_x = U\sin\theta + V\cos\theta \tag{1}$$

$$w_z = V\sin\theta - U\cos\theta \tag{2}$$

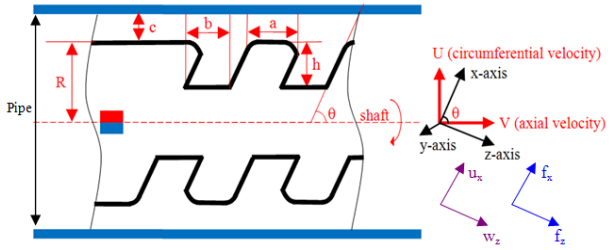

Figure 2. Conceptual structure of the screw thread

In the previous study, based on hydromechanical lubrication theory and Newton viscous law, the similar force analysis had been discussed [19]. According to our designed microrobot in the pipe, the main force will be evaluated as shown in the Table Ⅰ in the horizontal direction, which consists of f_x ,f_z, F_{axial}, F_{circum} $f_{l\text{-}resist}$ and $f_{r\text{-}frication}$. And in the vertical direction, the G and F_u should be considered separately.

TABLE I. Explanation of the Main Force

Main force	Explanation
f_x	The total shear stress of the screw thread gap region and the thread region in x-axis.
f_z	The total shear stress of the screw thread gap region and the thread region in z-axis.
F_{axial}	The axial traction force.
F_{circum}	The circumferential friction force.
$f_{l\text{-}resist}$	The resistance from the liquid.
$f_{r\text{-}friction}$	The rolling friction between the mircrobot and pipe
G	The weight of the microrobot

According to Newton viscous law, we can obtain the f_x and f_z as following:

$$\begin{aligned} f_x &= \mu A\frac{du}{dy} \\ &= -n\mu(U\sin\theta + V\cos\theta)\left(\frac{a}{c}+\frac{b}{c+h}\right) \end{aligned} \tag{3}$$

where n is the number of thread unit, μ is the viscosity coefficient of the liquid, A is the contact area, du/dy is the velocity gradient.

$$f_z = -n\mu w_z\left[\frac{3abh^2}{bc^3 + a(c+h)^3} + \frac{a}{c} + \frac{b}{c+h}\right] \tag{4}$$

Then we can compute the axial traction force, circumferential friction force, resistance from liquid as following:

$$\begin{aligned} F_{axial} &= f_x\cos\theta + f_z\sin\theta \\ &= \frac{3n\mu abh^2(U\sin\theta\cos\theta - V\cos^2\theta)}{bc^3 + a(c+h)^3} - n\mu V\left(\frac{a}{c}+\frac{b}{c+h}\right) \end{aligned} \tag{5}$$

$$\begin{aligned} F_{circum} &= f_z\cos\theta - f_x\sin\theta \\ &= \frac{3n\mu abh^2(U\cos^2\theta - V\sin\theta\cos\theta)}{bc^3 + a(c+h)^3} + n\mu U\left(\frac{a}{c}+\frac{b}{c+h}\right) \end{aligned} \tag{6}$$

$$\begin{aligned} F_{\text{l-resist}} &= 0.5k\rho V^2 S \\ &= 0.5k\rho V^2\pi R^2 \end{aligned} \tag{7}$$

$$F_{r-fricition} = \eta G \tag{8}$$

$$G = m_g g \tag{9}$$

$$F_u = \rho g V_g = \frac{\rho}{\rho_g}G \tag{10}$$

where k is the damping coefficient of the liquid, ρ is the density of the liquid, S is the front of contact area of the microrobot, η is the coefficient of rolling friction, G is the weight of the microrobot, V_g is the volume of the microrobot, ρ_g is the density of material used to design the microrobot.

We can obtain m_g from an electronic balance, and calculate G and F_u easily.In order to simplify the equations, we assumed β=a /a+b, γ=h/c, so we can obtain:

$$\begin{aligned} \overline{F}_{axial} &= F_{axial}\cdot\frac{c}{a+b} \\ &= \frac{3n\mu\beta(1-\beta)\gamma^3(U\sin\theta\cos\theta - V\sin^2\theta)}{(1-\beta)+\beta(1+\gamma)^3} - nV\mu\left(\beta+\frac{1-\beta}{1+\gamma}\right) \end{aligned} \tag{11}$$

$$\begin{aligned} \overline{F}_{circum} &= F_{circum}\cdot\frac{c}{a+b} \\ &= \frac{3n\mu\beta(1-\beta)\gamma^3(U\cos^2\theta - V\sin\theta\cos\theta)}{(1-\beta)+\beta(1+\gamma)^3} + nU\mu\left(\beta+\frac{1-\beta}{1+\gamma}\right) \end{aligned} \tag{12}$$

Therefore, the total force of the microrobot in the horizontal direction in-pipe is:

$$F_{horizontal} = \overline{F}_{axial} + \overline{F}_{circum} - F_{l-resist} - F_{r-friction} \tag{13}$$

In the vertical motion, the microrobot is also influenced by its gravity and the buoyancy from the liquid, we assumed $\Delta F = F_u - G$, so the total force of the microrobot in the vertical direction in-pipe is:

$$\begin{aligned} F_{vertical} &= \overline{F}_{axial} + \overline{F}_{circum} + \Delta F - F_{l-resist} - F_{r-friction} \\ &= F_{horizontal} + \Delta F \end{aligned} \tag{14}$$

When the traction force is zero, the axial speed is maximal, the expression of maximum speed as following [18]:

$$\begin{aligned} V_{\max} &= \frac{3n\beta(1-\beta)\gamma^3\sin\theta\cos\theta}{\left(\beta+\frac{1-\beta}{1+\gamma}\right)\left[(1-\beta)+\beta(1+\gamma)^3\right]+3\beta(1-\beta)\gamma^3\sin^2\theta}\cdot U \\ &= f(\beta,\gamma,\theta) \end{aligned} \tag{15}$$

B. *The motion analysis of the microrobot in the horizontal direction*

We had simulated the performance effect of the spiral angle θ to F_{axial}, F_{circum}, $f_{l\text{-}resist}$, $f_{r\text{-}friction}$, $F_{horizontal}$ and V_{max}. By refer to the structure of microrobot we designed, we assumed β=0.5, γ=1, μ=1, U=0.005, V=0.05, n=5, k=1, ρ=1, R=0.003. Considered of the size of the microrobot, we fixed the range of θ is 0° to 90°. The simulation results in the horizontal direction as shown in Fig. 3 and Fig. 4.

From the results, we conclude that when θ is 20° to 70°, F_{axial} the traction force of capsule is positive. Since the cross-sectional area of microrobot relative to the pipeline is very small, the affection of $f_{l\text{-}resist}$ is very small. In addition, when θ is equal to 45°, the microrobot can obtain the maximum total force and moving speed in the horizontal direction.

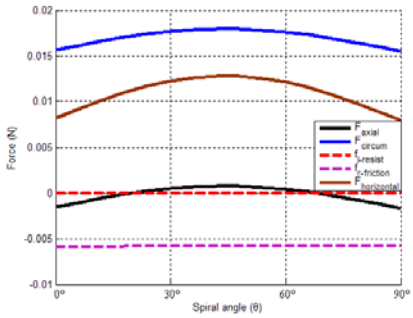

Figure 3. The curves of F_{axial}, F_{circum}, $f_{l\text{-}resist}$, $f_{r\text{-}friction}$, $F_{horizontal}$ when θ changes

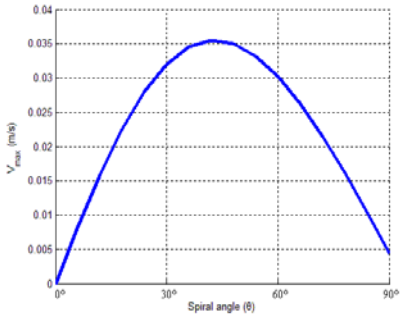

Figure 4. The curve of V_{max} when θ changes

C. *The motion analysis of the microrobot in the vertical direction*

We had also simulated the performance effect of the spiral angle θ in the vertical direction. We assumed β=0.5, γ=1, μ=1, U=0.005, V=0.05, n=5, k=1, ρ=1, ρ_g=1.1, R=0.003. Considered of the size of the microrobot, we fixed the range of θ is 0° to 90°. The simulation result is shown in Fig. 5.

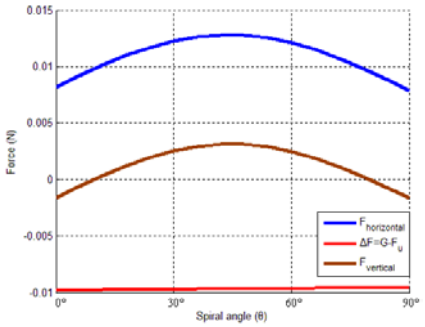

Figure5. The curves of $F_{vertical}$ when θ changes

From (14) and simulation result, we can find that $F_{vertical}$ is just related to $F_{horizontal}$ and ΔF, and when θ is from10° to 80°, the $F_{vertical}$ is a positive value, but it is a very small. So the microrobot can achieve upward motion without gravity compensation in theory. When θ is 45°, the microrobot can obtain the maximum total force 3mN in the vertical direction.

III. EXPERIMENTS ON THE PROPOSED MICROROBOT

A. *Experiment on forward-backward motion*

In the detection process, the microrobot should complete forward-backward motion in the pipe. Base on the theoretical analysis of the proposed microrobot [18], so we developed this new kind of spiral type microrobot, it as shown in Fig. 6 and the design parameters of it is shown in Table Ⅱ.

TABLE II. SPECIFICATION OF THE PROPOSED MICROROBOT

Size	Φ6mm×50mm
Weight	1.38g
Material of the body	EVA (Ethylene Vinyl Acetate)
Permanent magnet	1 piece

Figure 6. Prototype of the microrobot

By using the measurement system as shown in Fig. 7, with the aided of the laser displacement sensor system, the following characteristics of the moving speed were measured. We carried out the experiments by changing the frequency of input currents from 0Hz to 18Hz, and the amplitude of input currents were fixed at 0.7A.

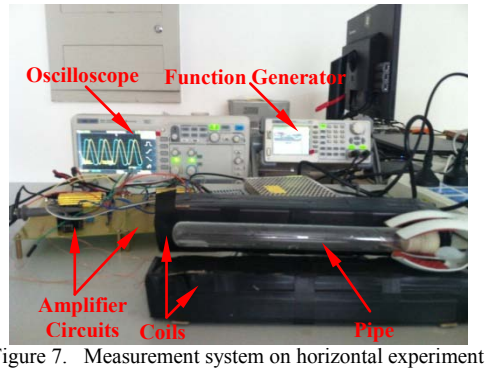

Figure 7. Measurement system on horizontal experiment

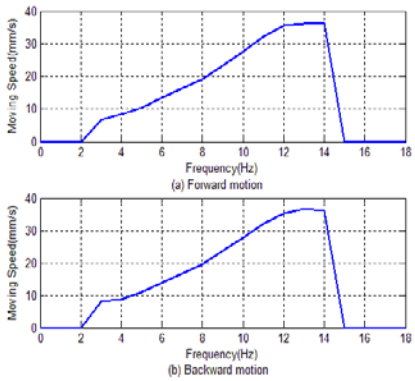

Figure 8. Moving speed of forward-backward motion

Based on the measurement system, the microrobot can achieve rotation motion in the pipe forward-backward. Through changing the frequency and phase of input currents [18], the experimental results of average moving speed of the microrobot were obtained as shown in Fig. 8.

Due to the completely symmetrical mechanical structure, we can find this kind of microrobots has the same kinematic characteristics in the horizontal direction. We have also obtained the maximum moving speed in the pipe is 36.5mm/s around 14Hz.

B. Experiment on upward-downward motion

According to our preceding analysis and the simulation results in Fig. 5, we can conclude that when θ is from10° to 80°, the $F_{vertical}$ is a positive value, but it is very small. When θ is equal to 45°, the microrobot can obtain the maximum total force 3mN in the vertical direction. Through the experiment on upward motion, it indicted that the microrobot can difficult realize the upward motion in the pipe with a very low speed. In addition, considered of simplify the control strategy, we should make the kinematic characteristics of the microrobot as symmetrical as possible, so we need counterweight for the microrobot in order to make ΔF=0, which is let the microrobot suspend in water.

Considered the material of the microrobot, we select another material that has a small density as gravity compensation. The specifications of materials are shown in Table Ⅲ and Fig. 9.

TABLE III. SPECIFICATIONS OF MATERIALS

Part	Main material	Density (g/cm3)
Body	EVA (Ethylene Vinyl Acetate)	1.1
Permanent magnet	NdFeB	6
Gravity compensation	EPE (Expandable Polyethylene)	0.003

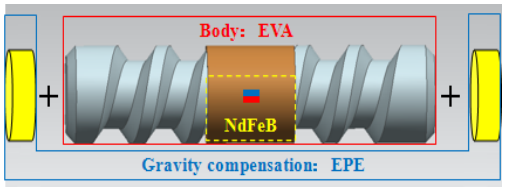

Figure 9. The gravity compensation of the microrobot

In addition, the EPE is a kind of very soft material, which installs at the head and end of the microrobot will buff the microrobot impact the pipeline, so that will improve the safety of detection process. The prototype of the microrobot with gravity compensation is shown in Fig. 10.

Figure 10. Prototype of the microrobot with gravity compensation

Based on the measurement system as shown in Fig. 11, the microrobot can achieve upward-downward motion in the pipe. Through changing the frequency and phase of input currents, the experimental results of average moving speed of the microrobot were obtained as shown in Fig. 12. We have also obtained the maximum moving speed in the pipe is 4.6mm/s around 16Hz.

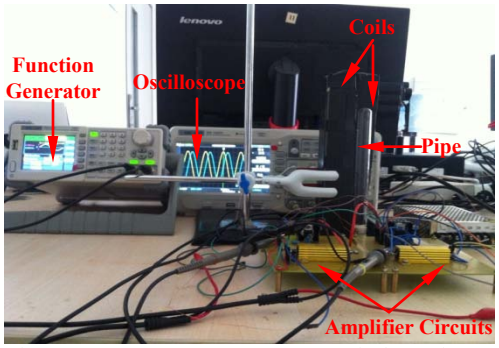

Figure 11. Measurement system on vertical experiment

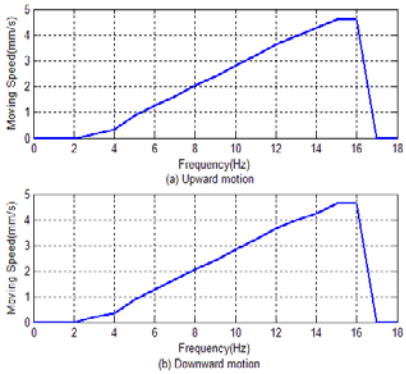

Figure 12. Moving speed of upward-downward motion

Seen from Fig. 8 and Fig. 12, it is finding that this kind of microrobots with symmetrical structure has the similar kinematic characteristics on the forward-backward and upward-downward motion. These symmetrical characteristics will make the control strategy much easier.

C. Experiments on developed microrobots with different spiral angles

We have evaluated the performance of the conceptual structure. In this paper, we defined the spiral angle is the angle between screw threads and shaft. We also had developed four types of microrobots with different spiral angles that 30°, 45°, 60° and 90°, which had the same length and thread unit numbers of spiral structure. The prototypes of the microrobot are shown in Fig. 13, and the specification of the spiral structures are shown in Table Ⅳ.

TABLE IV. SPECIFICATION OF PROTOTYPE MICROROBOTS

Type	Size	Spiral Depth	Spiral Angle
Microrobot 1	Φ5mm×50mm	3mm	90°
Microrobot 2			60°
Microrobot 3			45°
Microrobot 4			30°

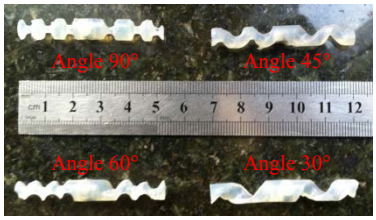

Figure 13. Prototypes of the microrobot with different spiral angles

Base on the experimental measurement system, we also measured the moving speeds of different spiral angles of the microrobots in the horizontal direction. By changing the frequency of the input currents from 0 Hz to 18 Hz, and the amplitude of input currents were fixed at 0.7A, the experimental results of average speeds were obtained as shown in Fig. 14.

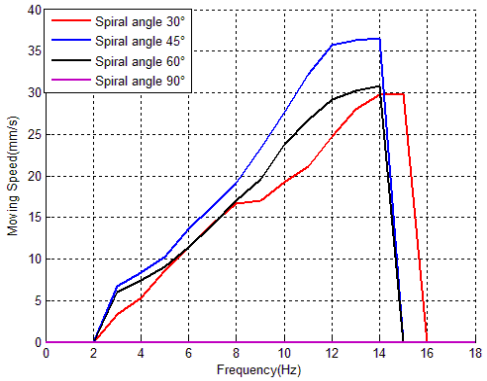

Figure 14. Moving speeds of the microrobots with different spiral angles

From Fig. 14, we can conclude that when the spiral angle is 90°, and the moving speed of the microrobot is nearly zero, because of there is no driving force in the motion direction. So the microrobot just does rotation motion in the pipe, without position changing. We can also find the kinematic characteristic of the spiral angle 30°, 45° and 60° are very similar, but just different from the maximum speed and moving frequency width. Due to the differences of mechanical structure of the spiral angles, the friction between microrobot and pipe is different, and the driving force from the spiral structure is also different.

When in a low frequency, the driving force cannot overcome its own gravity to drive the microrobots rotating in the pipe. So from 0Hz to 3Hz, the moving speed of the microrobots with spiral angle 30°, 45° and 60° is nearly zero. But when the frequency of the input currents over 4Hz, the microrobots begin to rotate with the rotation magnetic field in the pipe. Base on the spiral drive theory and previous analysis [19], the microrobots can be moving forward or backward in the pipe by changing the order of input currents. In addition, when the frequency of the input currents over 16Hz, the moving speed of the microrobots in pipe is down to zero. This is because the limitation of magnetic field intensity, the wireless microrobots can't rotate following the rotation magnetic field at a high level frequency any more, so the microrobots will out-of-step with the rotation magnetic field.

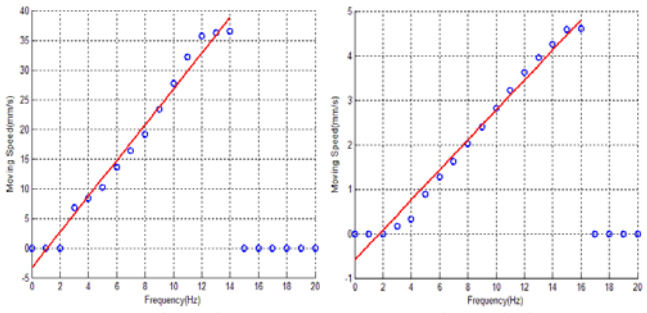

(a) Horizontal (b) Vertical

Figure 15. Moving speed fitting curves

We also fitted the speed curves of the kind of microrobots with 45° spiral angles, and the moving speed equations (16) and (17) for microrobot in the horizontal and vertical direction can be obtained from the fitting curves as shown in Fig. 15.where f is the frequency of input currents, v is the moving speed of the microrobot in pipe.

$$v_{Horizontal} = 3.0136f - 3.3515 \quad (16)$$

$$v_{Vertical} = 0.337f - 0.5925 \quad (17)$$

where f is the frequency of input currents, v is the moving speed of the microrobot in pipe.

IV. Design of Control Panel for the System

At the experimental stage, we usually use a function generator to generate sine wave signals, but this way is not portable and compact. Based on the experimental results, we design a control panel for our system.

The control panel we designed is shown in Fig. 16. Through selection of the buttons, we input the status we needed, and then the MCU will output the corresponding signals to the amplifying unit and display the current status. The control panel can realize stopping, running and changing the direction of motion, which can be selected through the button control as shown in Fig. 17. In the running status, we can choose low-speed motion, mid-speed motion and high-speed motion, and the moving speed can be referenced by the experimental results.

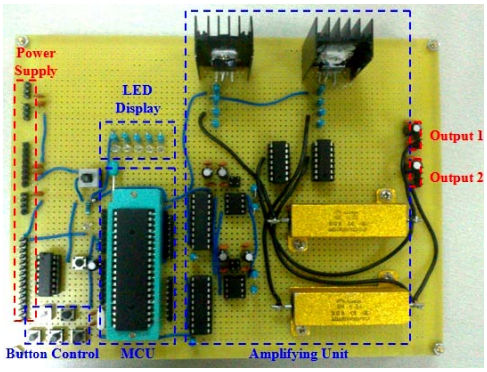

Figure 16. Control panel

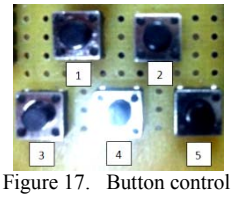

Figure 17. Button control
(1.Start/ Stop, 2.Motion direction control, 3.Low-speed motion, 4.Mid-speed motion, 5.High-speed motion)

According to the actual operation needs, we referenced our experimental results, and defined low-speed, mid-speed, high-speed motion as the following Table Ⅴ.

TABLE V. Motion State

Motion State	Frequency Selected	Speed of Horizontal Motion	Speed of Vertical Motion
Low-speed	4 Hz	8.32 mm/s	0.32 mm/s
Mid-speed	9Hz	23.3 mm/s	2.4 mm/s
High-speed	14 Hz	36.54 mm/s	4.26 mm/s

Base on the control panel, we measured the moving speeds of three motion states of the microrobot. The average results had been shown in Fig. 18.

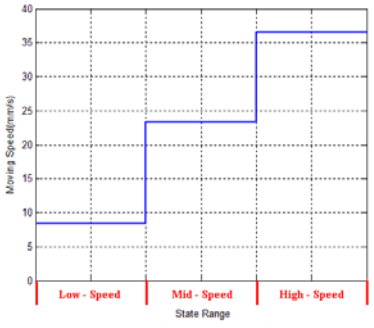

(a) Horizontal result

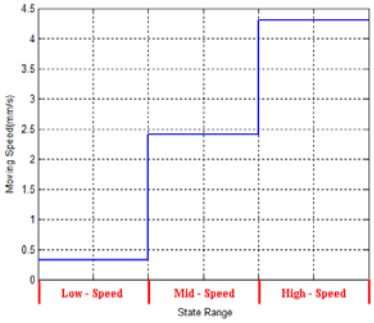

(b) Vertical result

Figure 18. Experimental results in three motion state

With this control panel, our system will be portable and compact, and we can control the microrobot current motion states intuitively and easily.

V. Conclusion and Future Work

In this paper, a new kind of wireless microrobots in pipe with symmetrical spiral structure has been developed. This paper has discussed the modeling and analysis the wireless microrobot structure. In order to evaluate the performance of the spiral structure, we also developed microrobots with different spiral angles. The experimental results indicated that the microrobot could achieve forward-backward, upward-downward motion in the pipe, and could stop at any position we needed. The maximum moving speed is 36.5 mm/s at the frequency of 14 Hz in the horizontal direction and 4.6 mm/s at the frequency of 16Hz in the vertical direction with currents of 0.7A based on the type of Mircorobot 3, which is the optimal structure with gravity compensation.

This kind of microrobots has the similar kinematic characteristics in the pipe, so the control strategies become much simpler. In order to realize portable and compact control, we designed a control panel, which can achieve stopping, running and changing the direction of motion. And in the running status, we can choose low-speed motion, mid-speed motion and high-speed motion.

In the future, we will focus on reducing the volume of the microrobot, and make it suitable for a more small space to work. It is also need to establish a more DOFs experimental system to realize the microrobot more DOFs motion in the pipe.

Acknowledgment

This research is supported by Key Research Program of the Natural Science Foundation of Tianjin（13JCZDJC26200）and General Research Program of the Natural Science Foundation of Tianjin (13JCYBJC38600).

References

[1] S. Sudo, S. Segawa, T. Honda, “Magnetic Swimming Mechanism in a Viscous Liquid”, Journal of Intelligent Material Systems and Structures, Vol.17, No.8-9, pp.729-736, 2006.

[2] K B. Yesin, K. Vollmers, B J. Nelson, “Modeling and Control of Untethered Biomicrorobots in a Fluidic Environment Using Electromagnetic Fields”, International Journal of Robotics Research, Vol.25, No.5-6, pp.527-536, 2006.

[3] G. Iddan, G. Meron, A. Glukhovsky, and P. Swain, “Wireless capsule endoscopy,” International Journal of Nature, Vol.4, pp. 717-719, 2000.

[4] M. Sendoh, K. Ishiyama, and K. I. Arai, “Direction and individual control of magnetic micromachine,” Proceedings of the IEEE Transactions on Magnetics, vol. 38, pp.3356–3358, 2002.

[5] Y Zhang, H Xie, N Wang, “Design, analysis and experiments of a spatial universal rotating magnetic field system for capsule robot,” Proceedings of 2012 IEEE International Conference on Mechatronics and Automation, pp.998-1003, 2012.

[6] Tan R, Liu H, Su G, “Experimental investigation of the small intestine's viscoelasticity for the motion of capsule robot,” Proceedings of the 2011 IEEE International Conference on Mechatronics and Automation, pp.249-253, 2011

[7] T. Honda, T. Sakashita, K. Narahashi, et al. “Swimming properties of a bending-type magnetic micro-machine”. Journal of Magnetics Society of Japan, Vol. 25, No. 4-2, pp.1175-1178, 2001.

[8] T Mei, Y Chen, G Fu and D Kong, “Wireless Drive and Control of a Swimming Microrobot”, Proceedings of the 2002 IEEE International Conference on Robotics and Automation, Vol.2, pp.1131-1136, 2002.

[9] M. Nokata, H. Masuka, S. Kitamura, “New magnetic rotational drive by use of magnetic particles with specific gravity smaller than a liquid”, Proceedings of the 2010 IEEE International Conference on Robotics and Automation, pp.2177-2182, 2010.

[10] S Guo, Y Sasaki, Fukuda T, “A New Kind of Microrobot in Pipe Using Driving Fin”, Proceedings of the 2003 IEEE/ASME International Conference on Advanced Intelligent Mechatronics, Vol. 2, pp.667-702, 2003.

[11] S Guo, Q Pan, “Mechanism and Control of a Novel Type Microrobot for Biobiomedical Application”, Proceedings of the 2007 IEEE International Conference on Robotics and Automation, pp.187-192, 2007.

[12] S Guo, Q Pan, Khamesee M B. “Development of a novel type of microrobot for biobiomedical application”, Journal of Microsystem Technologies, Vol.14, No.3, pp.307-314, 2008.

[13] Q Pan, S Guo. “A Paddling type of microrobot in pipe”, Proceedings of the 2009 IEEE International Conference on Robotics and Automation pp.2995-3000, 2009.

[14] Q Pan, S Guo, Okada T, “A Novel Hybrid Wireless Microrobot”, International Journal of Mechatronics and Automation, Vol.1, No.1, pp.60-69, 2011.

[15] Okada T, S Guo, Yamauchi Y. “Design of a wireless hybrid in-pipe microrobot with 3 DOFs”, Proceedings of the 2011 IEEE International Conference on Mechatronics and Automation, pp.1356-1361, 2011.

[16] T Okada, S Guo, N Xiao, “Control of the wireless microrobot with multi-DOFs locomotion for medical applications”, Proceedings of 2012 IEEE International Conference on Mechatronics and Automation, pp.2405-2410, 2012.

[17] Y Zhang, K Zhang, L Zhang, “Spiral drive characteristics of a micro robot inside human body,” International Journal of Robot, Vol. 28, pp.560-570, 2006.

[18] J Guo, S Guo, X Wei, “Development of a New Kind of Magnetic Field Model for Wireless Microrobots”, Proceedings of the 2013 ICME International Conference on Complex Medical Engineering, pp.580-585, 2013.